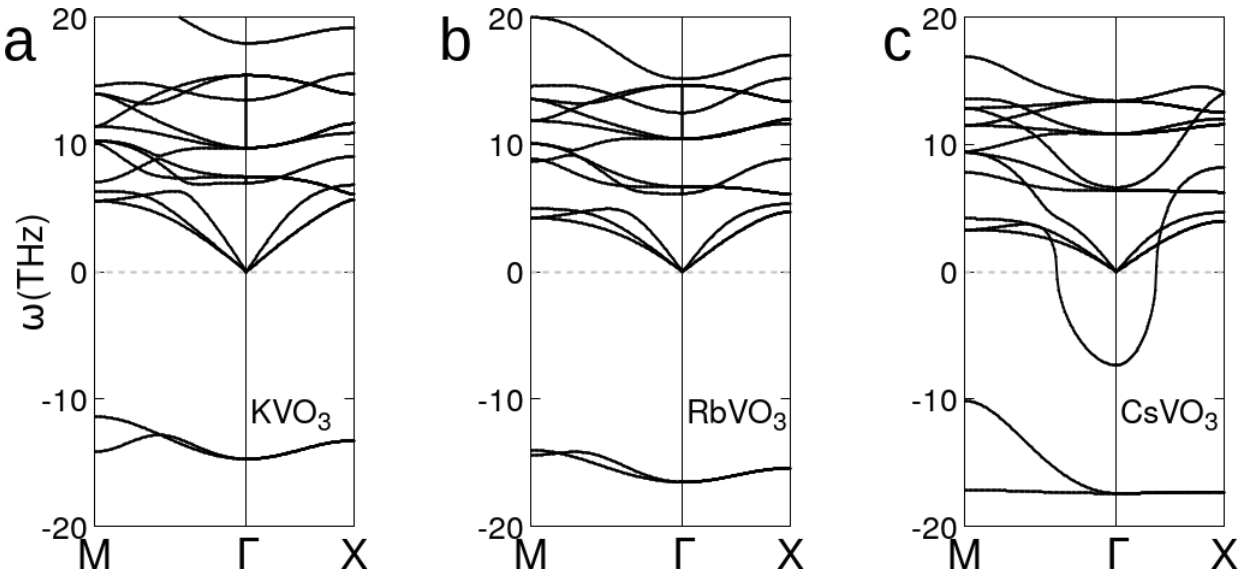

Supplementary Figure 1. **Phonon dispersions of the studied vanadates**. Phonon dispersion calculated in the cubic perovskite phase for KVO_3, $RbVO_3$ and $CsVO_3$ -**a**, **b** and **c**, respectively-. The three vanadates show strong polar and antipolar instabilities, being the latter less favourable in all cases.

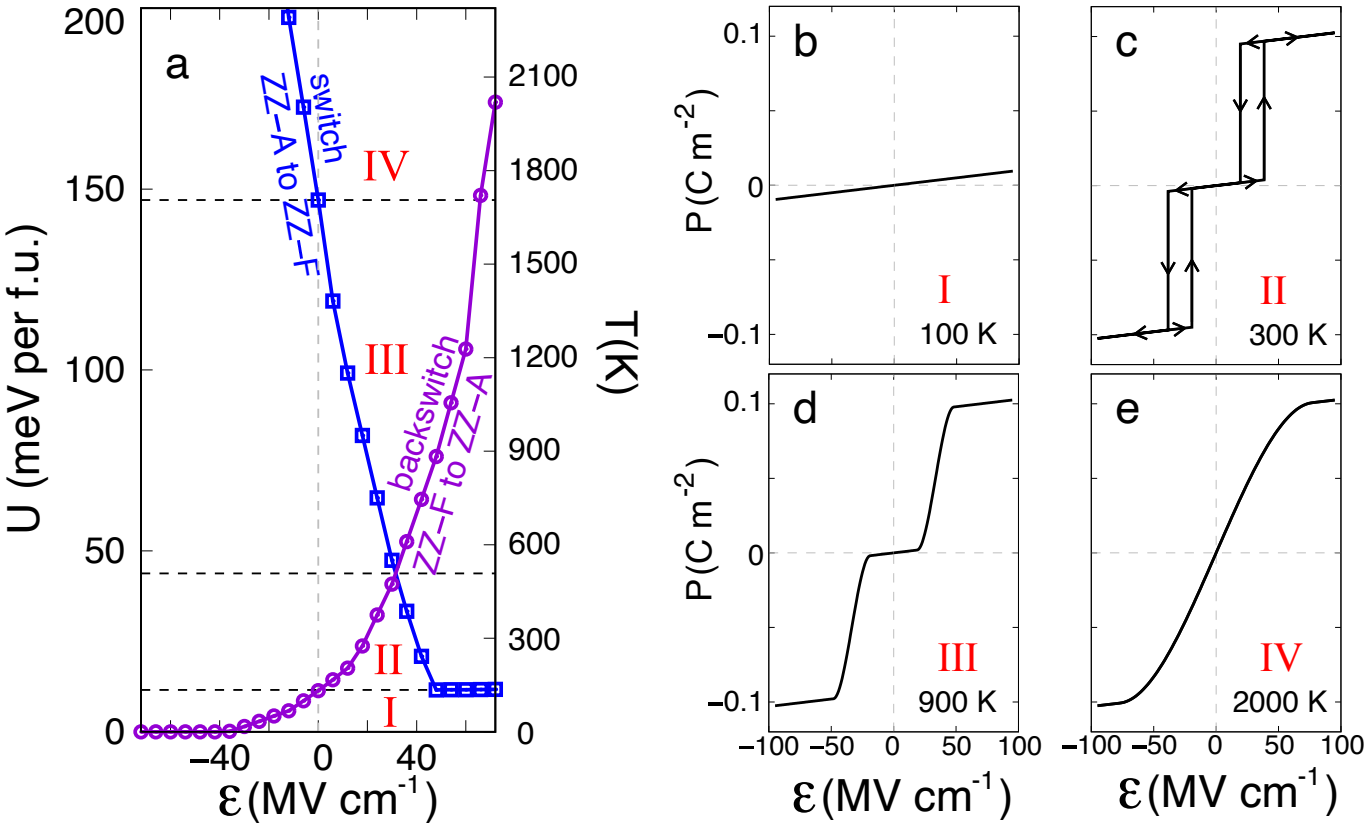

Supplementary Figure 2. **Largest energy barrier for switching and backswitching in KVO_3 and estimated hysteresis diagrams for different temperatures**. **a** Largest energy barrier *per* formula unit for switching from ZZ-A to ZZ-F (blue squares) and for backswitching from ZZ-F back to ZZ-A (purple circles) as a function of out-of-plane electric field. The horizontal dashed lines indicate the delimiting energies for regimes I to IV. The corresponding temperature scale is shown on the right. The behaviour of the polarisation with the electric field is shown at representative temperatures for regimes I, II, III and IV in panels **b**, **c**, **d**, and **e**, respectively.

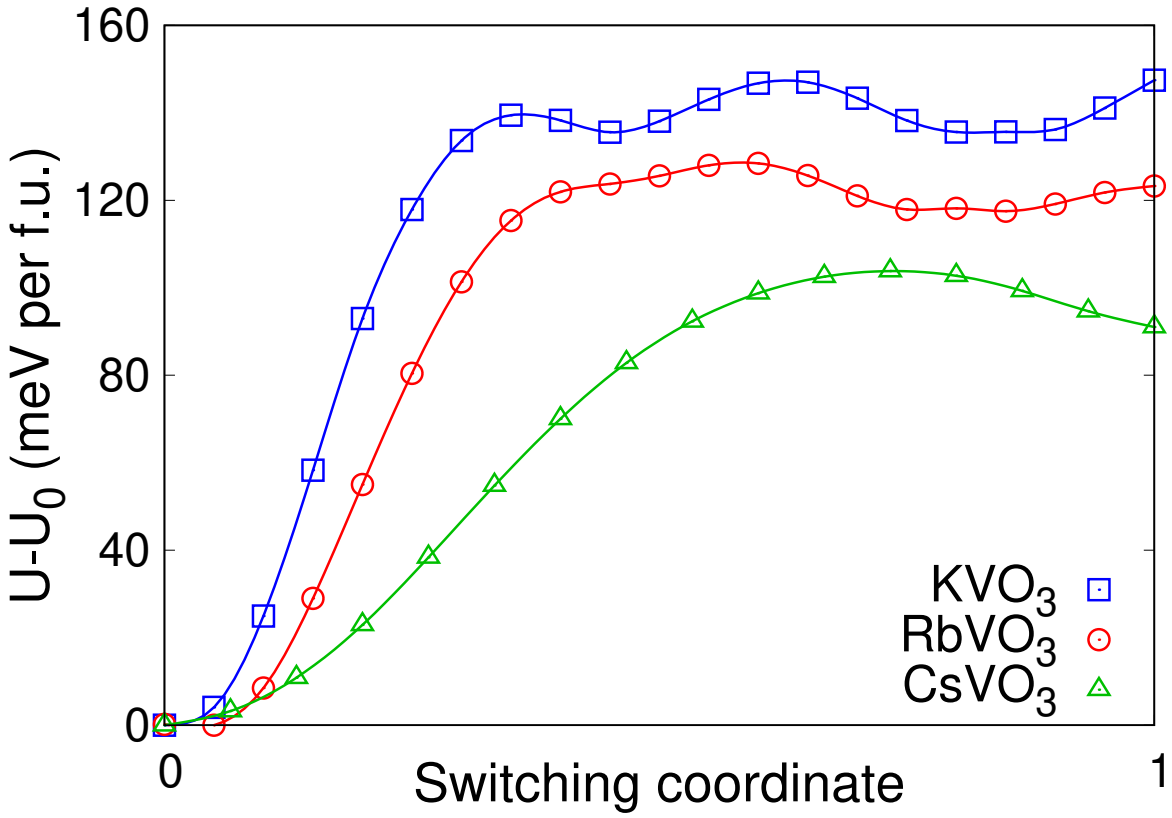

Supplementary Figure 3. **Minimum energy switching path for the studied vanadates**. Energy along the continuous path between the ZZ-A and ZZ-F states for KVO_3, $RbVO_3$ and $CsVO_3$ (blue, red and green lines, respectively) as obtained with the NEB method.

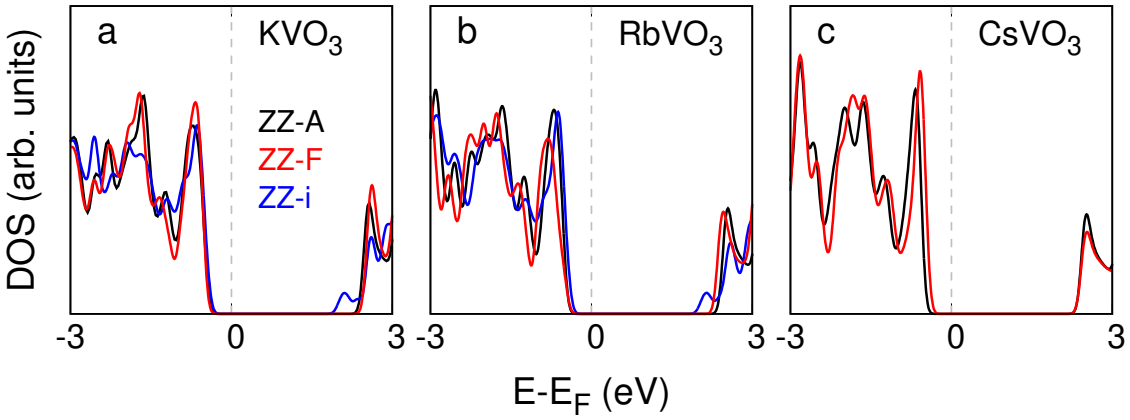

Supplementary Figure 4. **Densities of states of the studied vanadates**. Densities of states for KVO_3, $RbVO_3$ and $CsVO_3$ -**a**, **b** and **c**, respectively- in the ZZ-A, ZZ-F and ZZ-i phases (black, red and blue lines, respectively). The ZZ-i phase of $CsVO_3$ is not included because it is not stable.

SUPPLEMENTARY NOTES

Supplementary Note 1: High-throughput study of phonon instabilities

We conduct a high-throughput study of the phonon dispersion of several ABO_3 compounds in the cubic perovskite structure. We study non-magnetic materials to avoid additional complications in the analysis. The list of studied compounds is formed by $A_{\rm I}B_{\rm V}$ oxides with $A_{\rm I}$=Na, K, Rb, Cs, Ag and $B_{\rm V}$=V, Nb, Ta; $A_{\rm II}B_{\rm IV}$ oxides with $A_{\rm II}$=Ca, Sr, Ba, Pb and $B_{\rm IV}$=Ti, Zr, Hf; $A_{\rm III}B_{\rm III}O_3$ with $A_{\rm III}$ and $B_{\rm III}$=Sc, Y, La, Ac; and others ($SrXO_3$ with X=Ge, Sn, Pb, WO_3 $LaAlO_3$ and the non-oxide perovskites $CsPbY_3$ with Y=F, Cl, Br, I). The key quantities we track are the phonon instabilities at the centre of the Brillouin zone and at the Brillouin zone boundaries, looking for materials in which at least one antipolar instability (i.e. and instability involving displacements of the A or B cations lying at a zone boundary) is stronger than (or at least close in energy to) the polar one.

Of the more than 50 compounds studied, none presented a leading antipolar instability. A few of them, namely the alkali vanadates AVO_3 (A=K, Rb, Cs) show large antipolar instabilities almost as strong as the leading polar instability (see Supplementary Fig. 1). All three of them show a very flat band across the Brillouin zone connecting the polar instability (imaginary modes at Γ) with the antipolar instabilities (imaginary modes at zone boundaries M and X), the latter being less favourable. This is typical of ideal (Kittel-like) antiferroelectric materials, as for example discussed in a recent publication by Milesi-Brault *et al.*[1], and could have implications for the character of the phase transition (which can be expected to be of the order-disorder type).

Supplementary Note 2: Hysteresis diagram

To compute the hysteresis diagrams, we used the data displayed in Fig. 3a in the main article to calculate the largest energy barrier for KVO_3 to switch (ZZ-A $\rightarrow$ ZZ-F) and to backswitch (ZZ-F $\rightarrow$ ZZ-A) as a function of electric field. The results are shown in Supplementary Fig. 2. Four regimes can be identified as a function of the activation energy.

For activation energies below 12 meV per formula unit (f.u.) the system can not overcome the switching barrier, and thus the electric response would be similar to that of a paraelectric material (see Supplementary Fig. 2b).

At activation energies between 12 meV per f.u. and 45 meV per f.u. it is always possible to switch the system, and the switching field is larger than the backswitching field. In this regime, whose behaviour is depicted in Fig. 3b in the main text and in Supplementary Fig. 2c, the system will switch to the ZZ-F state at a large enough field (between $\sim$ 30 MV cm^{-1} and $\sim$ 45 MV cm^{-1}, depending on the activation energy). Once in the ZZ-F state, it will remain there until the field is lowered enough for the system to overcome the backswitching barrier. (For negative fields the response is symmetric since the initial state is antipolar and therefore centrosymmetric.) Overall the polarisation undergoes a double-hysteresis loop with the applied field.

For activation energies between 45 meV per f.u. and 147 meV per f.u. the behaviour of the system is qualitatively different, and is shown in Supplementary Fig. 2d. Starting from the ZZ-A ground state at zero field, once the switching field is reached, the system always has enough energy to overcome the backswitching barrier too. Therefore, between the switching and backswitching fields the system will gradually transient between the ZZ-A and the ZZ-F states. Hence, the hysteresis disappears.

Finally, for activation energies above 147 meV per f.u. the system can spontaneously transient between ZZ-A and ZZ-F at zero field. Therefore, the behaviour of the intermediate case discussed previously is extended up to zero field.

Note that, when computing the hysteresis diagrams, we did not take into account a possible partial switching to the ZZ-i ferrielectric state, but rather only complete switching and complete backswitching. In regime II intermediate states might be accessible, showing partially switched (or backswitched) polarisation, particularly for KVO_3 and $RbVO_3$ in which the ZZ-i state is metastable (see Supplementary Fig. 3).

In order to estimate the temperatures at which these regimes occur, we assume one vibrational degree of freedom per VO_4 tetrahedron, corresponding to the vibrational mode of the tetrahedron rotating about the chain. The addition of the average potential and kinetic energies yields a total thermal energy of k_BT per f.u. The resulting temperature scale is shown on the right axis in Supplementary Fig. 2a, and is the one employed in the main text. With this assumption we obtain that the temperatures delimiting regimes I and II, II and III, and III and IV are 140 K, 520 K and 1700 K, respectively.

Supplementary Note 3: Switching path for other vanadates

We compute the switching path between the ZZ-A and the ZZ-F state also for $RbVO_3$ and $CsVO_3$ and compare them to that of KVO_3. The results are displayed in Supplementary Fig. 3. The intermediate ZZ-i state is not metastable for $CsVO_3$ and only marginally stable for $RbVO_3$, probably due to the large size of the A cation as compared to KVO_3. For $RbVO_3$ the switching takes place in two steps, following essentially the same path as KVO_3. In contrast, in $CsVO_3$ all the tetrahedra of the rotating chain involved in the switching flip simultaneously, probably due to the lack of stability of the intermediate ZZ-i state. This suggests that the switching path may also be acted upon with A cation substitution The energy barriers also decrease with increasing A cation, as does the energy difference between the ZZ-A and ZZ-F states.

Supplementary Note 4: Densities of states

We compute the densities of states (DOSs) for the three vanadates around the Fermi level. The results are displayed in Supplementary Fig. 4 for the three relevant phases ZZ-A, ZZ-F and ZZ-i (black, red and blue lines, respectively). All the compounds are insulating in the three phases.

---

[1] Cosme Milesi-Brault, Constance Toulouse, Evan Constable, Hugo Aramberri, Virginie Simonet, Sophie de Brion, Helmuth Berger, Luigi Paolasini, Alexei Bosak, Jorge Íñiguez, and Mael Guennou, "Archetypal soft-mode-driven antipolar transition in francisite $Cu_3Bi(SeO_3)_2O_2Cl$," Phys. Rev. Lett. **124**, 097603 (2020).